Field Crops Research 318 (2024) 109613

Contents lists available at ScienceDirect

Field Crops Research

journal homepage: www.elsevier.com/locate/fcr

Optimizing deficit irrigation and fertilizer application for off-season maize production in Northern Benin

M. Gloriose B. Allakonon [a,*,1], Pierre G. Tovihoudji [a,2], P.B. Irénikatché Akponikpè [a,b,3], C.L. Bielders [c,4]

[a] Laboratory of Hydraulics and Environmental Modeling (HydroModE-Lab), Faculty of Agronomy, University of Parakou, 03 BP: 351, Parakou, Benin
[b] Institute of Science and Technology for Innovation in Africa (ISTI-Africa), Parakou, Benin
[c] Earth and Life Institute (ELI), Université catholique de Louvain, Ottignies-Louvain-la-Neuve 1348, Belgium

ARTICLE INFO

Keywords:
Sensitivity analysis
Crop models
CERES-Maize
Growing degree days
Food security

ABSTRACT

Context: Soil water and fertility management have been the main challenges of crop production in West Africa, and their impacts are exacerbated by climate variability. While research has been conducted to optimize fertility and water applications for rainfed crops production in this region, little is known about the management of these resources for off-season cereal crops production.
Objective: This study assessed the optimal combination of irrigation and fertilizer levels for off-season maize production in Benin, using the DSSAT CERES-Maize crop model.
Methods: Two years' experiments (2018 and 2019) of 4 levels of deficit nutrient (DN) and two years' experiments (2019 and 2020) of 4 levels of deficit irrigation (DI) were conducted and data were collected on maize growth and yield. DSSAT model was calibrated using crop data from DN experiment in 2018 (DN2018) and DI experiment in 2019 (DI2019), and validated using the DN2019 and the DI2020 experimental data. Then, a long-term scenarios analysis (40-years, 1980–2019) was performed to optimize (i) DI levels, (ii) DN rates; and (iii) combined DI levels and DN rates.
Results: The model predicted the grain yield (GY) and total aboveground biomass (TB), with a relative root mean square error and a coefficient of efficiency of 18.3 % and 0.38 for the GY and 11.7 % and 0.50 for the TB during the validation, respectively. However, the model did not account for the effects of DI or DN on the phenological dates, which led to similar predicted values for the anthesis and maturity dates among DI and DN treatments during calibration and validation. Moreover, the model was sensitive to periods with high values of temperature (>45°C) recorded during the DI period, inducing a reduction of the grain filling rate in DI treatments. DI treatments were more sensitive to a change in DUL, SLL, SAT, RGFIL and RUE than the DN treatments; while the DN treatments were more sensitive to the CTCNP2. Reducing maize water requirements by 40 % at the vegetative stage resulted in similar predicted grain yield as in the full irrigation treatment; while reducing the water requirements by 60 % resulted in similar predicted water use efficiency (WUE) as in the full irrigation treatment. Furthermore, the inter-annual variability of grain yield was lower under the optimal DI combined with no fertilizer but higher under high DI combined with higher fertilizer rates. Finally, a combination of 40–60 % of deficit irrigation at the vegetative stage and one-third to half of the recommended fertilizer rates depending on resources availability was the optimum combination of DI and DN rates for off-season maize production.
Conclusions: The projected grain yield and WUE under optimal DI and DN levels were likely underestimated due to shortcomings in the model structure to deal with effects of water and nutrient stresses on phenological dates. For reliable assessments of the effects of water and nutrient stresses on grain yield and WUE, there is need to update parameterization and code of the CERES crop models in DSSAT to have a sufficiently strong effect of water and nutrient stress on phenological dates, and the contribution of phenology to LAI and yields predictions.

* Corresponding author.
E-mail addresses: gallakonon@gmail.com (M.G.B. Allakonon), pierretovihoudji@yahoo.fr (P.G. Tovihoudji), charles.bielders@uclouvain.be (C.L. Bielders).
[1] https://orcid.org/0000-0002-3832-716X
[2] https://orcid.org/0000-0002-4352-3923
[3] https://orcid.org/0000-0001-9195-6240
[4] https://orcid.org/0000-0003-2865-4236

https://doi.org/10.1016/j.fcr.2024.109613
Received 23 December 2023; Received in revised form 8 October 2024; Accepted 8 October 2024
Available online 19 October 2024

1. Introduction

Africa is emerging as the continent with the highest demographic growth rate, and a population projected to double by 2036, and to represent 20 per cent of the world population by 2050 (United Nations, 2009). Feeding this growing population is and will continue to be a concern, particularly in environments where high climatic uncertainties pose an additional challenge to crop production. In Benin, the spatio-temporal variability of rainfall limits the rainfed cereal cropping systems, like the maize cropping systems. Rainfall uncertainties such as dry spells, late onset of rainy season, shortening of raining season, etc., lead to crops yield losses (Yabi and Afouda, 2012; Agbossou et al., 2012). Short cycle maize varieties of 60–90 days are cultivated two to three times during the cropping season in order to adapt to erratic rainfall seasons (Tidjani and Akponikpè, 2012; Allé et al., 2014; Yegbemey et al., 2017). In addition to the adoption of short cycle varieties, off-season maize production supported with irrigation could also be an adaptive strategy to the erratic rainfall seasons, but this remains unexplored in Benin.

In Benin, likewise major cereal crops, maize is traditionally cultivated in the rainfed season, with a growing window spanning from April to September. Consequently, researches have focused on the rainfed growing season, with little investigations on the possibilities of growing cereals crops in off-season using irrigation. Off-season crop production involves the cultivation of crop during the dry season, where water is supplied to crops through irrigation. The application of full irrigation water during the dry season increased maize yield to 4.8 Tons ha^{-1} in Togo, based on a simulation approach (Gadédjisso-Tossou et al., 2018). Furthermore, off-season production increased agricultural revenues since farmers can harvest the crops at least twice a year (Badabaté et al., 2012). In this study, off-season maize production is addressed as an adaptation strategy to erratic rainfall and as a potential means of improving food security in a context of climate variability.

Climate projections depict a decreasing trend of annual rainfall, but an increasing trend of annual temperature ranging from 0.8°C by 2030 to 2.3°C by 2050 over Benin. These projections are expected to lead to maize yield reduction in the range of 17 % by 2030 and 30 % by 2050 (Direction Générale de l'Environnement et du Climat, 2022). The predicted decreasing trend of rainfall suggests that off-season production of crops should use water resources sustainably in order to increase both crop water and irrigation water productivity. Deficit irrigation (DI) is a strategic water management practice that supplies water below the full crop water requirement (Geerts and Raes, 2009; Fereres and Soriano, 2007). Specifically, DI can induce insignificant yield losses, when applied reasonably, by considering the sensitivity of crop's growth stages. In a review study, Allakonon and Akponikpè (2022a), reported that a mild deficit irrigation level below 20 % led to 0.5–17.45 % of yield loss in the vegetative stage of grain maize crop, compared to 46 % of yield loss in the reproductive stage. Similarly, the irrigation water use efficiency and the crop water use efficiency under DI varies with the crop's growth stage. DI is also recognized as an adaptation strategy of irrigated crop systems to improve crop water productivity in limited water availability conditions (Allakonon et al., 2022b; Gomaa et al., 2021). In this study we assumed that the implementation of optimized deficit irrigation levels would enhance irrigation and crop water productivity compared to full irrigation levels for off-season maize production.

Beside rainfall uncertainties, cereal crop production is also limited by soil fertility depletion in Benin. Generally, farmers are recommended to apply a certain amount of fertilizer for maize production. However, they hardly apply the recommended rates due to lack of resources. Recent studies have recommended viable long-term and cost-effective nutrient rates for maize production systems in Benin. Tovihoudji et al., (2019) reported that one-third of the recommended fertilizer rate could be the optimal fertilizer rate that guarantees a long-term minimum grain yield with little inter-annual yield variability in northern Benin. Nevertheless, recommendations of fertilizer rates for maize production have been made essentially for rainfed maize systems, with little regards towards off-season irrigation maize systems. In this study, we address the identification of optimal fertilizer and irrigation rates, as well as the optimal combination rates of these inputs for a sustainable off-season maize production in Northern Benin.

Crop models have been used to support decision making regarding management practices (Song and Jin, 2020; Tofa et al., 2020; Dhillon et al., 2020). They can conceptualize complex agricultural systems in a simplest way, in a short time and require only minimum experiments compared to results generated from long term experiments. The Decision Support System for Agrotechnology Transfer (DSSAT) crop model has been used to simulate efficiently maize growth, soil water, and N-balance under diverse management conditions in West Africa, including in Benin (Dzotsi et al., 2003; McCarthy et al., 2012; Adnan et al., 2017; Igué et al., 2013; Amouzou et al., 2018). In this study, the DSSAT crop model is used to identify the optimal combination of deficit irrigation and fertilizer rates for off-season maize production in Benin.

2. Material and methods

2.1. Study area

This study was conducted from 2018 to 2020 on the experimental site of the Faculty of Agronomy, University of Parakou, Benin. The experimental site is located at 9°20'08.8" N latitude, and 2°38'54" E longitude, 347 m a.s.l. in the agroecological zone III (Zone vivrière du Sud-Borgou) (MEPN, 2008), and is representative of the dry-sub-humid climate regime based on the UNEP classification system. The 40-years (1979–2019) annual average rainfall of Parakou is 1105 mm. The soil of the experimental site is loamy sand in texture, acid, and rich in nitrogen and phosphorus in the upper 0-40 cm layers.

2.2. Field experiment

Two deficit irrigation (DI) and two nutrient deficit (DN) experiments were carried out in a randomized complete block experimental design (RCBD), with three replications. Both experiments types were conducted on a 90-days cycle maize crop variety, the EVDT-97-STR-W. The DI experiments were conducted in 2019 (DI2019) and in 2020 (DI2020), and consisted of four DI treatments defined based on the daily crop evapotranspiration (ET_c): (i) optimal irrigation (DI_0) with a daily application of 100 % ET_c; (ii) DI_{25} with 75 % ET_c; (iii) DI_{50} with 50 % ET_c; and (iv) DI_{75}, with 25 % ET_c. Daily maize ET_c was estimated from CROPWAT V8.0 (FAO, 1992). The total irrigation amount for DI_0, DI_{25}, DI_{50} and DI_{75} treatments was 472 mm, 442 mm, 412 mm and 388 mm, in the DI2019 experiment; and 392 mm, 377 mm, 349 mm, and 335 mm in the DI2020 experiment, respectively. Deficit irrigation was intentionally applied from 31^{rst} days after sowing (DAS) to 50^{th} DAS in all DI treatments. In addition, full crop water requirement was applied from sowing to 30^{th} DAS, and from 51^{th} DAS to crop maturity. For both DI2019 and DI2020 experiments, sowing occurred after a total irrigation event of 25 mm for each. The DI experiments received the recommended NPK fertilizer rates in both 2019 and 2020 growing seasons.

The DN experiments were conducted during the 2018 and 2019 rainfall seasons, and consisted in applying 4 fertilizer rates based on the recommended fertilizer rates (RFR): (i) the control with no fertilizer (F_0), (ii), one-third of the RFR (F_1), 62.5 kg NPK (15−15−15) + 31.25 kg urea (46 %) ha^{-1}, (iii) half of the RFR (F_2), 100 Kg NPK + 50 Kg urea ha^{-1}, and (iv) the recommended fertilizer rate (F_3), 200 Kg NKP and 100 kg urea ha^{-1}. These rates are equivalent to: 23.8 kg of nitrogen (N) ha^{-1}, 4.1 kg of phosphorus (P) ha^{-1}, and 7.8 kg of potassium (K) ha^{-1} for F_1; 38 Kg N ha^{-1}, 6.5 Kg P ha^{-1}, and 12.5 Kg K ha^{-1} for F_2; and 76Kg N ha^{-1}, 13.1 Kg P ha^{-1} + 24.9 Kg K ha^{-1} for F_3. For both DI and DN experiments, NPK (15-15−15) fertilizer was applied on 15^{th} DAS and the urea was applied on 45^{th} DAS, after ploughing. Irrigation was applied to all DN experiments when rainfall was absent for three consecutive days, to avoid water stress in DN experiments. A total irrigation amount of 39 mm and 71 mm was applied during the DN2018 and DN2019 experiments, respectively. Plant thinning was performed manually to 2 plants hill^{-1} to reach a planting density of 62,500 plants ha^{-1} in all DI and DN experiments, ten days after sowing

2.3. Modeling approach

2.3.1. DSSAT model description

2.3.1.1. CERES-MAIZE module. The Decision Support System for Agrotechnology Transfert (DSSAT-CSM) has been designed with the aim to (i) simulate monocrop production systems in one or multiple seasons and in rotations with minimum input data, (ii) provide a platform for easily incorporating modules for other biotic and abiotic factors, (iii) provide a platform for comparing alternative modules for model improvement, evolution and documentation, and (iv) provide the capability to use the crop system module into other programs in a modular way. More details on the structure of the crop model are given in Jones et al. (2003). DSSAT is a dynamic and predictive model that has mechanistic, and deterministic components. Mechanistic, because it can explain the behavior of a system at an upper integration level by considering processes of a lower integration level and represents the system structure. Dynamic, because it can represent a crop system with time dimension, and deterministic, because the predicted values do not depend on probability distribution (Jones and Kiniry, 1986).

The CERES-Maize (Crop Environment Resource Synthesis-Maize) crop module (Jones et al., 2003) in DSSAT model version 4.7.5 was used for the simulation (Hoogenboom et al., 2019). We used the Priestley and Taylor/Ritchie (Priestley and Taylor, 1972) method to compute the potential evapotranspiration, which requires only the daily solar radiation and temperature as input, compared with the Penman-FAO and the Penman-Montheit methods. The potential evapotranspiration is computed in the soil-plant-atmosphere module of the model. The USDA-Soil Conservation Services method (USDA-Soil Conservation Service, 1972) was chosen to simulate soil water infiltration, and the Ritchie soil water balance model was used for computing drainage, based on a 'tipping bucket' approach. These processes are computed daily in the soil water module. Furthermore, the daily canopy photosynthesis method (Jones et al., 1989) was selected to simulate daily photosynthesis and the CENTURY method for soil Organic Carbon and nitrogen dynamics (Gijsman et al., 2002). The daily canopy photosynthesis predicts daily gross photosynthesis as a function of daily radiance for a full canopy, which is then multiplied by factors 0 or 1 for light interception, temperature, leaf nitrogen status, and water deficit. More details on all methods used are given in Jones and Thornton (2003).

2.3.1.2. Conceptualization of water stress in DSSAT crop model. Water stress acts on transpiration and radiation use efficiency, leaf expansion that determines above ground growth, and leaf senescence. The fundamental principle for estimating water stress in DSSAT is the comparison between potential transpiration (demand) and potential root water uptake (plant extractable soil water, being the offer) (Anapalli et al., 2008). DSSAT accounts for the effect of water stress by computing two water stress factors, the TURFAC (Eq. (1)) and SWFAC (Eq. (2)). Under non-limiting water conditions, the maximum root water uptake is higher than the potential transpiration. As the soil water content decreases due to uptake, the maximum root water uptake decreases. When this decrease reaches a critical stage, TURFAC is activated. TURFAC is calculated using the formula (Anapalli et al., 2008):

$$\mathrm{TURFAC} = \mathrm{TRWUP} / (\mathrm{RWUEP1} * \mathrm{EP}_0) \quad (1)$$

where TRWUP is the potential root water uptake and RWUEP1 is a species-specific parameter which is given the value of 1.5 for all crops included in DSSAT, version 4.7.5 and EP_0 is the potential transpiration. When the RWUEP1 is less than 1, TURFAC is activated. TURFAC mainly affects the expansive crop growth details such as the internode elongation and the spread of the crop's leaves. The second stress factor called SWFAC affects crop phenology, growth and biomass-related processes. It is activated when potential transpiration demand equals or exceeds potential root water uptake, and it is defined as:

$$SWFAC = TRWUP / EP_0 \quad (2)$$

The value of both stress factors ranges from zero to one, where zero represents maximum stress and one represents no stress. The TRWUP (Eq. (3)) is defined as a function of soil water, soil properties, and root length density as follows:

$$\mathrm{TRWUP} = \frac{\mathrm{SWCON1} * \exp^{(\mathrm{MIN}((\mathrm{SWCON2}(\mathrm{SW_i} - \mathrm{LL_i}), \quad 40.)}}{\mathrm{SWCON3} - \ln \mathrm{LV_i}} \times \mathrm{Z_i} \times \mathrm{LV_i} \quad (3)$$

Where $\boldsymbol{LV_i}$ is the root length density (cm cm^{-3}), Z_i the thickness (cm), SW_i the soil water content (cm^3 cm^{-3}) and LL_i the lower limit of plant available water in soil layer i (cm^{3}cm^{-3}). SWCON1, SWCON2, and SWCON3 are soil water conductivity coefficients. SWCON1 is equal to 0.00132, SWCON2 = 120 − 250LL_i, and SWCON3 is equal to 7.01 in DSSAT version 4.6 (Song and Jin, 2020).

The DSSAT model has been calibrated under limited crop water conditions in different ways: (i) through the calibration of the crop genetic coefficients (Geng et al., 2017); (ii) the adjustment of the RWUEP1 coefficient (in the CANEGRO Model, Kapetch et al., 2016); (iii) the adjustment of the radiation use efficiency, RUE (Ma et al., 2011; Song and Jin, 2020); (iv) the calibration of soil hydraulic parameters such as the soil drained upper limit (SDUL), the soil lower limit (SLL), the soil water content at saturation (SAT), the soil drainage coefficient or soil water conductivity factor (SDRL or SWCON) and the soil saturated hydraulic conductivity (SSKS) (DeJonge et al., 2012; Ma et al., 2009). Here, only parameters to which the grain yield and $LAI_{max.}$ were sensitive, have been presented for the calibration in the results section (Fig. 6)

2.3.1.3. Conceptualization of nitrogen stress in DSSAT crop model. In the CERES-Maize model, a critical N concentration (TCNP) is defined as the lowest concentration at which maximum growth occurs, and a minimum N concentration (TMNC) is defined as the minimum concentration below which all growth ceases (Godwin and Singh, 1998). TCNP (Eq. (4)) is calculated as:

$$\mathbf{TCNP = 0{,}0.1*EXP}\ (\boldsymbol{CTCNP1\text{-}(CTCNP2 * Gstage)}) \quad (4)$$

Where CTCNP1 is the maximum N concentration, CTCNP2 a coefficient for change in concentration as a function of growth stage, and $\boldsymbol{G_{stage}}$, a non - integer growth stage indicator.

Nitrogen stress occurs when the actual N concentration (TANC) in plant tissue is lower than the critical N concentration level (TCNP). This can happen when there is N deficiency for metabolism maintenance or when there is N deficiency for a new growth. A N factor (NFAC) is defined, and ranges from zero when the N concentration is at TMNC, to unity when it is at TCNP or above. NFAC is thus the factor used in the simulation of the effect of N deficiency on growth processes (Godwin and Singh, 1998; Liu et al., 2012). But in practice, only the CTCNP1 and CTCNP2 coefficients are tuned to reflect the effect of nitrogen stress on crop growth in CERES-Maize.

In the occurrence of combined abiotic stresses such as water, nitrogen or temperature stress, the model considers the minimum of two or more values of a growth variable under different stresses.

2.3.2. Input files for DSSAT calibration and validation

2.3.2.1. Weather file. The Weatherman utility was used to create a weather file based on the daily rainfall, maximum and minimum air temperature and solar radiation over Parakou, for the period 1980–2020.

2.3.2.2. Soil file. Measured soil properties were used to create a soil file with the Soil Data tool, Table S1. The soil profile used for this simulation is presented in Table 1. The initial soil moisture values in 2018 were estimated by setting the date of start of simulation on the beginning of the year 2018 under fallow as antecedent crop. Then, the soil water content values around 140–150 days of the year were considered as the initial soil moisture before the start of rainfall. The initial soil moisture values are presented in Table S2. The runoff curve number (SLRO) and the drainage coefficients (SLDR) were set to *81* and *0.75* respectively. DSSAT computes the runoff curve using the USDA Soil Conservation Services curve number technique, which estimates the total runoff rate from the total daily precipitation. SLRO ranges from 0 (no runoff), to 100 (total runoff) based on land cover and soil type. The drainage coefficient (mm/day) represents the fraction of water between the actual water content and the drained upper limit that drains from a soil layer in one day and varies between 0 (no drained soils) and 1 (excessively drained soils). The root distribution factor (SRGF) was estimated based on a function in DSSAT: SRGF = 1 for layers above 15 cm, and SRGF = 1 * EXP (- 0.02 * LAYER_CENTER) for soil layers below 15 cm. SRGF ranges from 0 to 1.

Clay (%); Silt (%); Sand (%); BD: bulk density (g cm^{-3}); SLL: Lower limit (cm^3 cm^{-3}); DUL: drained upper limit (cm^3 cm^{-3}); SAT: saturated soil moisture content (cm^3 cm^{-3}); SSKS: soil hydraulic conductivity (cm h^{-1}); SRGF: soil root growth factor; NO_3^-: Nitrate (mg kg^{-1}); NH_4: Ammonium (mg kg^{-1}).

2.3.2.3. Cultivar coefficients files. The maize crop cultivar used was described by three types of files in DSSAT model: (i) the cultivar file, (.*cul)* that contains the values of crop genetic parameters; (ii) the ecotype file (.*eco*) that contains information on the ecotype to which belong a cultivar and (iii) the species file (.*spe*). Maize crop is characterized by six genetic parameters (Table 2) that describe its potential growth and yield.

2.3.2.4. Experiment files. The experiment file contains information related to the management practices that occurred from planting to harvesting in both DI and DN experiments. The calibration of DSSAT was carried out using the data collected during the DI2019 and the DN2018 treatments, while the validation was undertaken with the data from the DI2020 and the DN2019 treatments

2.3.2.5. Sensitivity analysis. A sensitivity analysis of soil fertility factors (CTCNP2, SLPF), soil water parameters (DUL, SLL, SAT, SSKS, SWCON, CN), radiation effect (RUE) and temperature effect (RGFIL) was conducted. The RMSE values of grain yield and maximum leaf area index ($LAI_{max.}$) were plotted against the variation in the values of each of these parameters.

The sensitivity to DUL, SLL and SAT was done using the DI2019 and DI2020 treatments (Fig. 6a, b & c). The sensitivity to the nitrogen stress factor (CTCNP2) was carried out considering the DN2018 and DN2019 treatments (Fig. 6d). Since the temperatures values recorded during the DI experiments were higher compared to the temperature during the DN experiments (Fig. 1C1 and 1C2), a sensitivity analysis was conducted for the factor that controls the temperature effect on relative grain filling rate (RGFIL), using the DI2019 and DI2020 treatments (Fig. 6e). This coefficient was set to *45.5*, to be higher than the maximum temperature recorded in the DI experiments. The sensitivity analysis to SLPF, SSKS, SWCON, CN and RUE was performed using both DI and DN treatments (Fig. S1).

Table 2
Initial guess and adjusted valued of maize cultivar coefficients.

Cultivar coefficients	Definitions	Initial guess[a]	Adjusted Values
P_1 (°C day)	Thermal time from seedlings emergence to the end of the juvenile phase (expressed in °C day, above a base temperature of 8°C) during which the plant is not responsive to changes in photoperiod	210.1 (130–380)	187.3
P_2 (days)	Extent to which development (expressed as days) is delayed for each hour increase in photoperiod above the longest photoperiod at which development proceeds at a maximum rate (which is 12.5 hours)	0.001 (0–2)	0.500
P_5 (°C day)	Thermal time from silking to physiological maturity (expressed in degree days above a base temperature of 8 °C).	600.1 (600–1100)	611.5
G_2 (number)	Maximum possible number of kernels per plant.	520.0 (400–1100)	600.0
G_3 (mg day^{-1-1})	Kernel filling rate during the linear grain filling stage and under optimum conditions (mg/day)	09.5 (4–11.5)	11.35
PHINT (°C day)	Phylochron interval; the interval in thermal time (degree days) between successive leaf tip appearances.	60 (30–90)	66

[a] : the genetic values of the initial guess were taken from a medium cultivar DMR calibrated by Tovihoudji et al., (2019), (P1 and P2). Values in parentheses are range of values from DSSAT/APSIM database for African cultivars and soils.

2.3.3. DSSAT calibration and validation

The calibration process was done in two steps. The first step consisted in the calibration of the maize cultivar genetic coefficients (Table 2), which characterize the phenology and growth of the cultivar. Six cultivar coefficients were calibrated automatically using the DSSAT-PEST package (Ma et al., 2020), developed to couple DSSAT and PEST for automatic optimization of crop genetic parameters. The PEST parameters used for the calibration are presented in Table S3. In total eight (08) measured growth variables from the DN2018 and DI2019 experiments were used to calibrate the genetic variables in the DSSAT-PEST package. These variables include: the anthesis date, the maturity date, the maximum LAI (LAI_{max} in m^2m^{-2}), the unit dry weight, which is the weight per unit grain (mg), the number of grains per cob, the grain yield at maturity (Kg ha^{-1}), the aboveground biomass (Kg ha^{-1}) and the harvest index. The second step consisted in the calibration of the nitrogen stress factor (CTCNP2) using treatments of the DN2018 experiment.

Table 1
Soil profile used for simulation.

Soil Layers (cm)	Clay	Silt	Sand	BD	SLL	DUL	SAT	SSKS	SRGF	NO_3^-	NH_4	pH
0–20	8.1	14.5	77.4	1.42	0.031	0.08	0.32	23	1	3.4	1.4	7.4
20–40	10.1	12.1	77.8	1.53	0.031	0.096	0.32	32.7	0.549	2.1	1.3	7.6
40–100	14.6	13.1	72.2	1.58	0.031	0.112	0.32	32.7	0.247	0.5	0.1	7.5

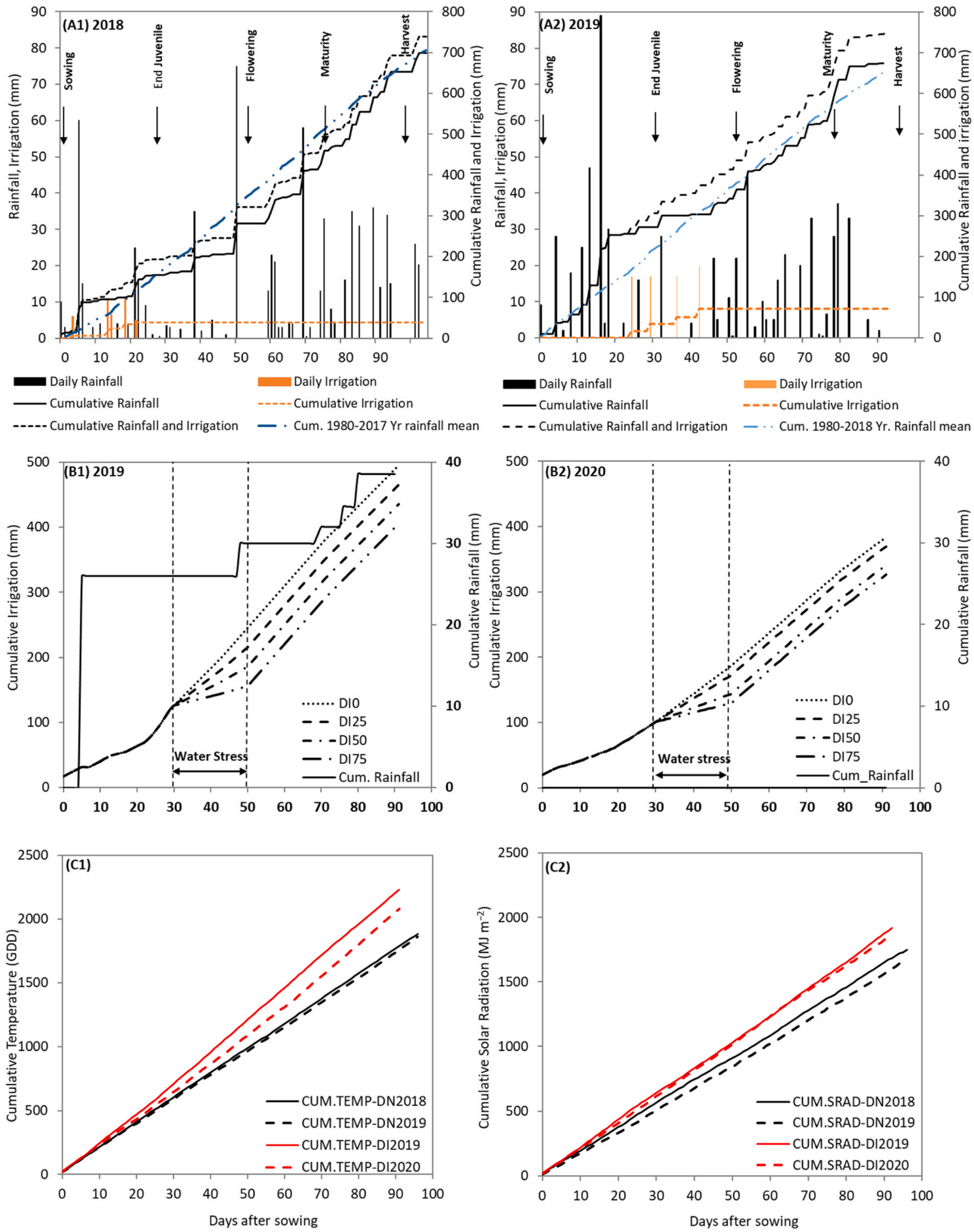

Fig. 1. Rainfall trends during DN2018 (A1) and DN2019 (A2) experiments; cumulative irrigation and rainfall during DI2019 (B1) and DI2020 (B2) experiments; cumulative temperature in growing degree days (C1) and cumulative solar radiation (C2) during DN and DI experiments (*2-column image; Online Version only for color*).

Then the species-specific parameter RWUEP1 has been calibrated using treatments of the DI2019 experiment.

The calibrated genetic coefficients, the CTCNP2 and the RWUEP1 have been validated using the treatments of the DI2020 and DN2019 experiments.

2.3.4. *Long-term scenario analysis*

A long-term experiment scenario analysis was run using the calibrated and validated DSSAT model, over 40 years (1980–2019) period. Three types of scenarios were considered for the long-term experiment simulations. The first scenario comprised eight (08) deficit irrigation levels (with 10 % increment of irrigation amount) at the vegetative stage from 31 DAS to 50 DAS as explained under the field experiment section. For this first type of scenario, sowing occurred during the dry season on 19th January each year and yield was harvested on 20th April. The second type of scenarios consisted in four fertilizer rates application as described for the DN experiments under the field experiment section. The third type of scenarios combined the eight deficit irrigation level (scenarios 1) with the four fertilizers rates applications (scenarios 2). For each type of scenario, initial soil conditions were reinitialized in the beginning to avoid residual long term effect of treatments from previous years.

2.4. Model performance evaluation

The accuracy of the CERES-Maize model's outputs was assessed with statistical indicators including the root mean square error (RMSE), in Eq. (5), (Willmott, 1981), the normalized or the relative root mean square error (nRMSE) in Eq. (6), the index of agreement (d) in Eq. (7), and the modified coefficient of efficiency (EF_1), in Eq. (8) (Yang et al., 2014).

$$RMSE = \left[\sum_{i=1}^{N} \frac{(Y_i - X_i)^2}{N}\right]^{1/2} \tag{5}$$

$$nRMSE = RMSE * 100/\overline{X} \tag{6}$$

$$d = 1 - \frac{\sum_{i=1}^{N} (Y_i - X_i)^2}{\sum_{i=1}^{N} (|Y_i - \overline{X}| + |X_i - \overline{Y}|)^2} \tag{7}$$

$$E_1 = 1 - \frac{\sum_{i=1}^{N} |Y_i - X_i|^2}{\sum |X_i - \overline{X}|^2} \tag{8}$$

Where I = 1, 2, …, N, is the i^{th} measurement, N the number of observations, Y the predicted value, X the observed value, $\overline{Y}$ is the mean of the predicted values, and $\overline{X}$ is the mean of the observed values. When predicted values fit exactly the observed values, RMSE and nRMSE are 0 and the corresponding d-value is 1. The nRMSE is used as a relative measure for inter comparisons of different variables or different models (Priesack et al., 2006) and the index of agreement, d ($0 \leq d \leq 1$), a dimensionless measure used to make cross-comparisons between simulated and observed data (Yang et al., 2014).

In addition to these statistical indicators, the overall accuracy of the predicted values was tested using the ordinary least squares analysis between the predicted and the observed values. The regression slope was generally significant when the p-value of the F-Test statistic was $<$ 0.05.

3. Results

3.1. Weather conditions during the experiments

The total annual rainfall was 1236.5 mm and 1699.3 mm in 2018 and 2019 and amounted to 653 mm and 680.5 mm during the DN2018 and DN2019 experiments, respectively (Fig. 1A1, A2). No rainfall occurred during the DI2020 experiment. However, the cumulative rainfall ranged from 17 mm to 198 mm, with an average of 84 ± 40 mm from sowing to harvest during the dry season between 1980 and 2019 (Fig. 1B1, B2).

The maximum daily temperature ranged from 28 °C to 36 °C, and from 27 °C to 36 °C for the DN2018 and the DN2019 experiments, respectively; while it ranged from 35 °C to 43 °C, and from 34 °C to 41 °C for the DI2019 and DI2020 experiments, respectively. The cumulative temperature in growing degree days (GDD) and the cumulative solar radiation were both higher for the DI experiments than the DN experiments (Fig. 1C1, C2).

3.2. Calibration of DSSAT

Overall, the calibrated genetic parameters resulted in a more accurate prediction of the anthesis dates (AD) and physiological maturity dates (PMD) for the DN2018 nutrient stress treatments, (nRMSE = 4 for both AD and PMD) compared to the deficit irrigation DI2019 treatments (nRMSE = 30 for AD, and 25.6 for PMD). The model predicted the AD and PMD with a RMSE of 2.1 and 3.3 respectively, for the DN treatments, and a RMSE of 18.4 and 24.1, respectively for the DI treatments (Table 3). The $LAI_{max.}$ was predicted with a RMSE value of 0.38 m^2m^{-2} for the DN2018 and 0.23 m^2m^{-2} for DI2019 treatments. The model predicted the time-series LAI with a RMSE ranging from 0.18 m^2m^{-2} for the DI_{25} treatment to 0.32 m^2m^{-2} for the DI_{75} treatment among DI treatments, and from 0.17 m^2m^{-2} for the F_0 treatment to 0.51 m^2m^{-2} for the F_2 treatment among the DN treatments. The d-index ranged from 0.84 to 0.98 during the calibration of the time-series LAI for all DI and DN treatments (Fig. 2). The model showed a satisfactory fit between predicted and observed values of grain yield, stover yield and aboveground biomass at harvest with respective nRMSE of 21.4 %, 18.5 %, 16.1 %, (Fig. 3b, c, and d, respectively). Moreover, the regression slopes between the predicted and measured values were statistically significant for all variables ($p<0,05$).

3.3. Validation of DSSAT

The predicted values of AD and PMD showed similar trend in the validation as in the calibration, with better fits for the DN compared to the DI treatments. The time-series LAI were validated with a RMSE ranging from 0.20 m^2m^{-2} for both the DI_{50} and DI_{75}treatments to 0.26 m^2m^{-2} for both the DI_0 and DI_{25}treatments among DI treatments, and from 0.17 m^2m^{-2} for F_1 treatment to 0.30 m^2m^{-2} for the F_3 treatment among DN treatments. Overall, the d-index ranged from 0.89 to 0.98 across the time-series LAI for all treatments used during the validation process (Fig. 2). The model over-estimated the predicted values of $LAI_{max.}$ for all treatments during the validation with a RMSE value of 0.23 m^2m^{-2} (Fig. 4).

The grain yield, stover yield and aboveground biomass were validated with RMSE values of 422.5 Kg ha^{-1}, 147.5 Kg ha^{-1} and 985.2 Kg ha^{-1} respectively. The coefficient of efficiency was higher for the aboveground biomass (0.5) than grain yield (0.38) and stover yield (0.30) (Fig. 5b, c and d). The linear regressions explained 97 % and 80 % of the total variance, indicating a good agreement between simulated and observed values of grain yield and total aboveground biomass, respectively.

3.4. Sensitivity analysis of the model to soil water parameters, nutrient stress factor and temperature factors

In general, a variation of the DUL, SLL and the SAT from their measured values either increased or stabilized the RMSE of grain yield and the $LAI_{max.}$, suggesting the measured values of DUL, SLL and SAT are the best fit for the simulations (Fig. 6a, b & c). The RMSE of the grain yield increased as the CTCNP2 increased or decreased, but the RMSE of the $LAI_{max.}$ did not vary (Fig. 6d). Thus, the CTCNP2 was maintained at 0.12 after the sensitivity analysis. The sensitivity analysis to the factor that controls the effect of temperature on relative grain filling rate (RGFIL) was conducted using the grain yield values only, since the RGFIL factor affects only the grain filling rate. Thus, an increase of RGFIL from 0 % to 60 % increased the RMSE of grain yield from 576 Kg ha^{-1} to 934 Kg ha^{-1}. A decrease of RGFIL by 50 % induced a two-fold increase of the RMSE of grain yield (Fig. 6e).

The RMSE of grain yield and $LAI_{max.}$ for both DN and DI treatments did not vary with the variation of the SSKS and the SWCON, suggesting the grain yield and the $LAI_{max.}$ were not sensitive to the SSKS (Fig. S1A) and the SWCON (Fig. S1B). Meanwhile the RMSE of grain yield of both DN and DI treatments increases as the runoff curve number (CN) increases but was stable as CN value decreases. However, the RMSE of the $LAI_{max.}$ did not vary with a variation of CN (Fig. S1C). The RMSE of grain yield increases by 20 % in the DI treatments, as a result of increase in

Table 3
Anthesis and physiological maturity dates during model calibration and validation.

Calibration	Treatments		F_o	F_1	F_2	F_3	DI_0	DI_{25}	DI_{50}	DI_{75}
	Growing seasons		2018				2019			
	Anthesis dates	Obs.	55	52	55	52	50	58	59	76
		Sim.	55	55	55	55	45	45	45	45
		PD	0	5.8	0	5.8	-10	-22.4	-23.7	-40.8
		RMSE	2.1				18.4			
		nRMSE	22.9							
	Maturity dates	Obs.	83	81	86	83	88	92	92	105
		Sim.	86	86	86	86	71	71	71	71
		PD	3.6	6.2	0	3.6	-19.	3–22.8	-22.8	-32.4
		RMSE	3.3				24.1			
		nRMSE	19.4							
Validation	Growing seasons		2019				2020			
	Anthesis dates	Obs.	55	54	53	52	52	57	58	75
		Sim.	55	55	55	55	47	47	47	47
		PD	0	1.8	3.8	5.7	−9.6	−17.5	−18.9	−37.3
		RMSE	1.9				16.04			
		nRMSE	20.0							
	Maturity dates	Obs.	84	81	83	80	90	96	100	109
		Sim.	87	87	87	87	74	74	74	74
		PD	3.6	7.4	4.8	8.7	−17.8	−22.9	−26.0	−32.1
		RMSE	5.2				25.7			
		nRMSE	20.5							

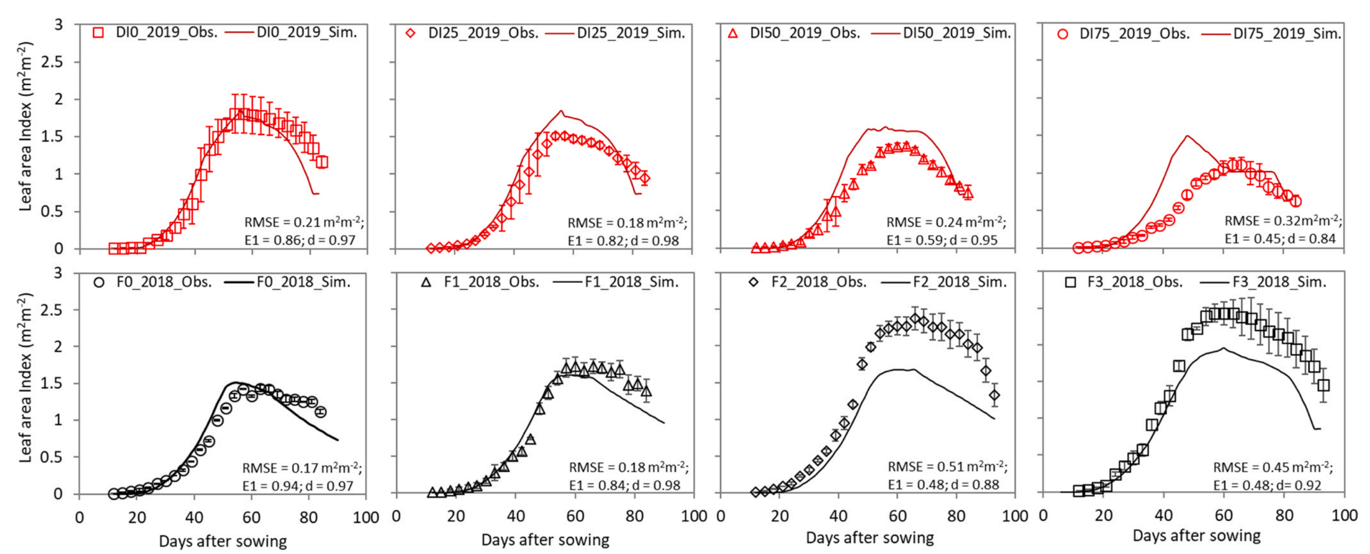

Fig. 2. Observed and simulated time-series leaf area index for maize during model calibration with the DN2018 (black curves) and the DI2019 treatments (red curves).

RUE value, implying that the grain yield in the DI treatments was more sensitive to the increase of RUE values compared to the DN treatments (Fig. S1D). Similarly, the RMSE of grain yield was two-times higher for the DI treatments than the DN treatments when SLPF increases by 50 %. As a result, the grain yield of DI treatments was more sensitive to an increase in SLPF, while the opposite trend was observed as SLPF decreases (Fig. S1F).

3.5. *Response of maize yield and water productivity to long-term scenario analysis regarding irrigation and fertilizer management*

3.5.1. *Long-term scenario analysis for Irrigation management*

Overall, the predicted grain and stover yields decreased with increasing deficit irrigation amount; and ranged from 1884 Kg ha^{-1} to 4006 Kg ha^{-1} for the DI_0 treatment and from 905 Kg ha^{-1} to 3049 Kg ha^{-1} for the DI_{80} treatment in the 1980–2019 period (Fig. 7a). However, the predicted average grain and stover yields were similar among DI_0, DI_{10}, DI_{20}, DI_{30} and DI_{40} treatments on the one side and between DI_{70} and DI_{80} treatments on the other side. Similar trends were observed for the predicted WUE, which decreased with increasing deficit irrigation amount. Maize WUE ranged from 4.0 Kg ha^{-1} mm^{-1} to 9.3 Kg ha^{-1} mm^{-1} for the DI_0 treatment, and from 2.3 Kg ha^{-1} mm^{-1} to 7.5 Kg ha^{-1} mm^{-1} for the DI_{80}, and was statistically identical between DI_0, DI_{10}, DI_{20}, DI_{30}, DI_{40}, DI_{50} and DI_{60} deficit irrigation treatments (Fig. 7b).

3.5.2. *Long-term scenario analysis for fertilizer management*

The long-term 40-year (1980–2019) simulations indicated that the grain yield consistently increased with increasing fertilizer rates, with average grain yield ranging from 2605 Kg ha^{-1} in the no fertilized treatment, F_0 to 4523 Kg ha^{-1} in the recommended fertilizer treatment, F_3 (Fig. 7c). Grain yield ranged from 2228 Kg ha^{-1} to 3020 Kg ha^{-1}; 3362 Kg ha^{-1} to 4409 Kg ha^{-1}; 3698 Kg ha^{-1} to 4965 Kg ha^{-1} and 3783

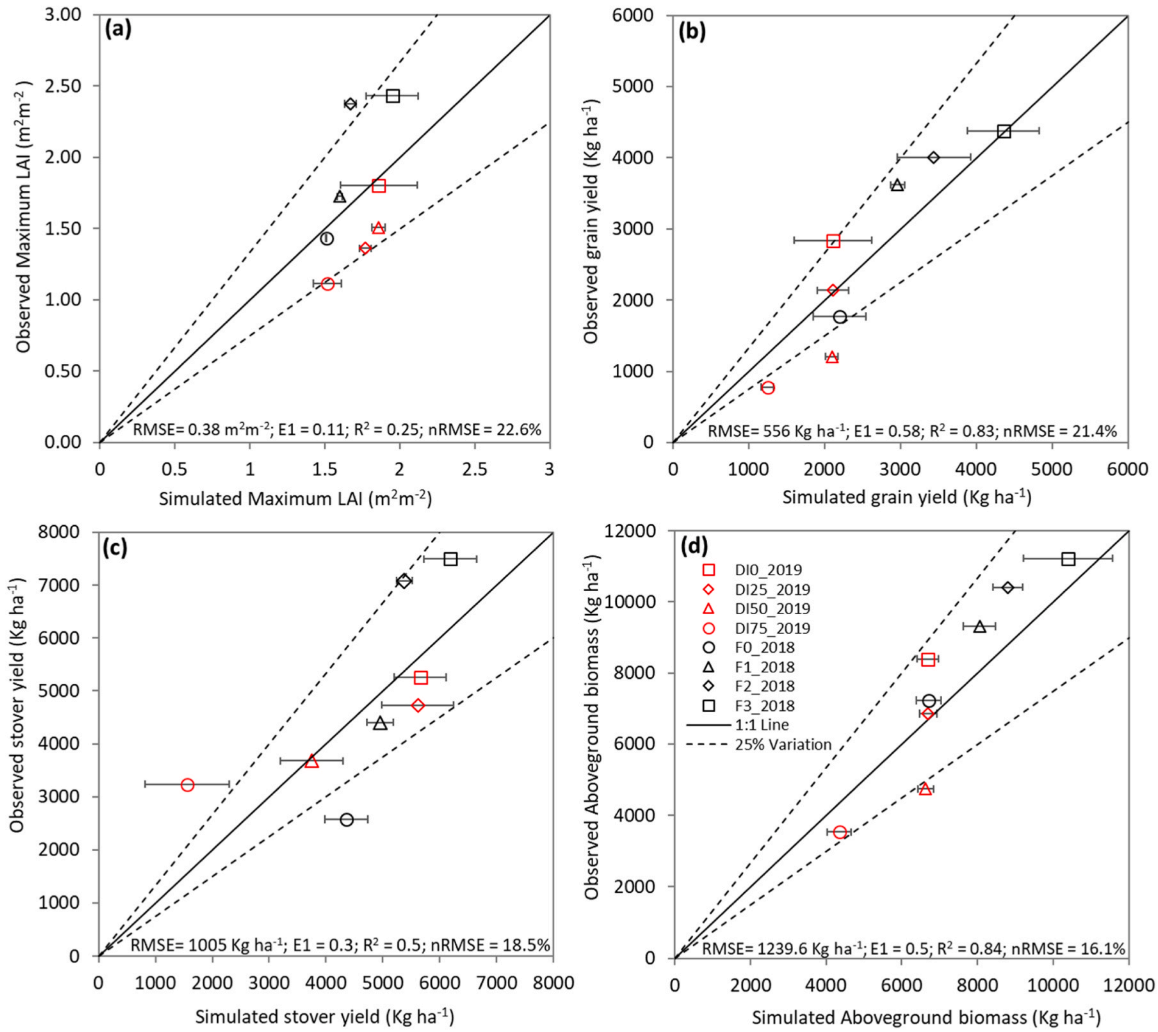

Fig. 3. Observed and simulated (a) maximum leaf area index, (b) grain yield at harvest, (c) stover yield at harvest and (d) total aboveground biomass at harvest of maize crop during model calibration using DN2018 (black color points) and DI2019 treatments (red color points).

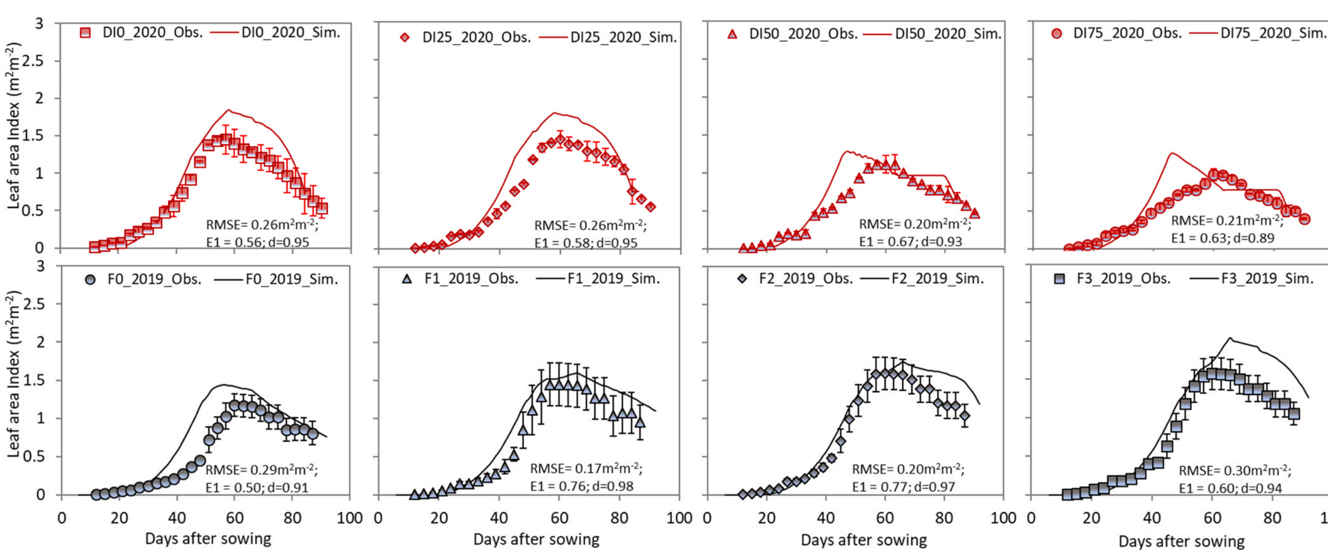

Fig. 4. Observed and simulated leaf area index for maize during model validation with the DN2019 treatments (black dots and curves) and the DI2020 treatments (red dots and curves).

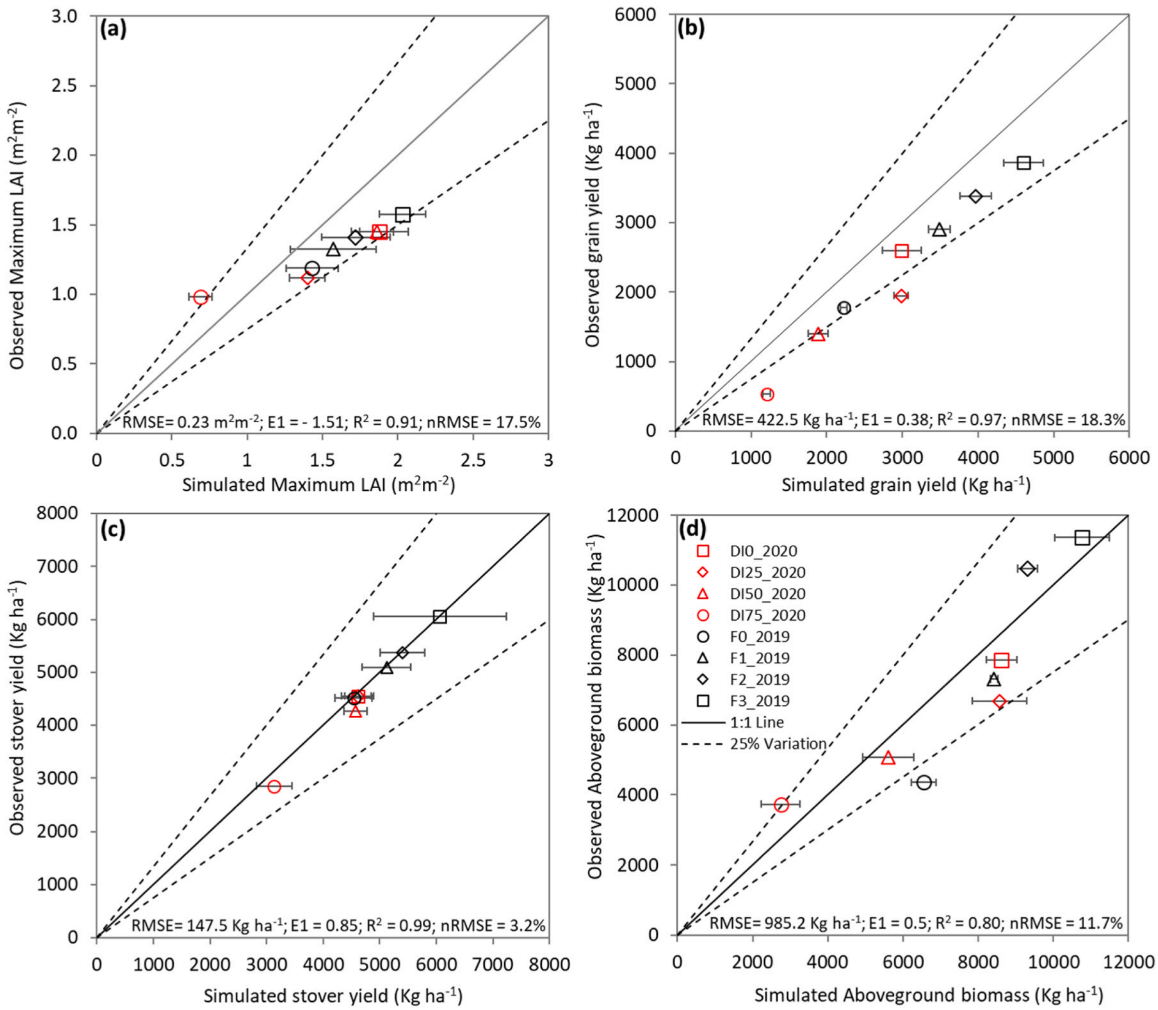

Fig. 5. Observed and simulated maximum leaf area index (a), grain yield at harvest (b), stover yield at harvest (c) and total aboveground biomass at harvest (d) of maize crop during model validation using DN2019 (black color points) and DI2020 treatments (red color points).

Kg ha^{-1} to 5282 Kg ha^{-1} in F_0, F_1, F_2 and F_3 treatments, respectively. The inter-annual standard deviation of grain yield, WUE and IWUE was lower for the F_0 treatment (Fig. 8), and higher for the F_3 treatment, specifically for DI30 to DI60 treatments.

3.5.3. Long-term scenario analysis for combined irrigation and fertilizer management

The long-term scenario analysis on combined irrigation and fertilizer management shows that the grain yield is similar among F_3, F_2 and F_1 treatments, as long as 60 % of the maize crop water requirement or more (DI_{40}) is satisfied. Grain yield under F_3 treatment decreases by 25 % when water stress from deficit irrigation increases from DI_{60} to DI_{70}, and by 32 % when water stress increases from DI_{60} to DI_{80} (Fig. 8a). The variability of grain yield is lower when optimal irrigation rate is applied without fertilizer but is higher when high water stress is combined with higher fertilizer rates (Fig. 8b).

Maize WUE and inter-annual variability of WUE followed similar trends with grain yield. WUE increases under combination of lower to middle DI rates (from DI_{20} to DI_{50}) and recommended fertilizer rates, but decreases under combination of high water stress and recommended fertilizer rates (Fig. 8c). the inter-annual variability of maize WUE is higher under combination of recommended fertilizer rates and middle DI levels (DI_{40} to DI_{60}). The irrigation water use efficiency (IWUE) tends to increase with increasing DI levels (from DI_{10} to DI_{30}) at all fertilizer rates. In opposite, lower fertilizer rates combined with high DI levels (DI_{60} to DI_{80}) induce a decrease in IWUE (Fig. 8e). The inter-annual variability of IWUE increases with increasing DI levels for all fertilizers treatments and is higher under the combination of recommended fertilizer rates and middle DI levels (DI_{40} to DI_{60}), (Fig. 8f).

4. Discussion

4.1. Maize yield predictions of DSSAT model under water and nitrogen stresses

The effect of water and nitrogen stresses on maize growth and yield was predicted with the DSSAT model, considering DI treatments monitored in dry seasons experiments on the one side, and DN treatments during the rainfed season experiment on the other side. Following the calibration of maize genetic coefficients, the model produced fair to good agreement between the simulated and observed grain yield, stover yield and aboveground biomass and the LAI_{max}. The nRMSE was in the order aboveground biomass < stover yield < grain yield < $LAI_{max.}$ during the calibration and in the order stover yield < aboveground biomass < $LAI_{max.}$ < grain yield during the validation, while the model efficiency coefficient followed the order $LAI_{max.}$ < stover yield < aboveground biomass < grain yield during the calibration and the order $LAI_{max.}$ < grain yield < aboveground biomass < stover yield during the validation. The correlation coefficient R^2 between the simulated and observed variables was in the order $LAI_{max.}$ < stover yield < aboveground biomass< grain yield during the calibration, and in the order aboveground biomass < $LAI_{max.}$ < grain yield < stover yield during the

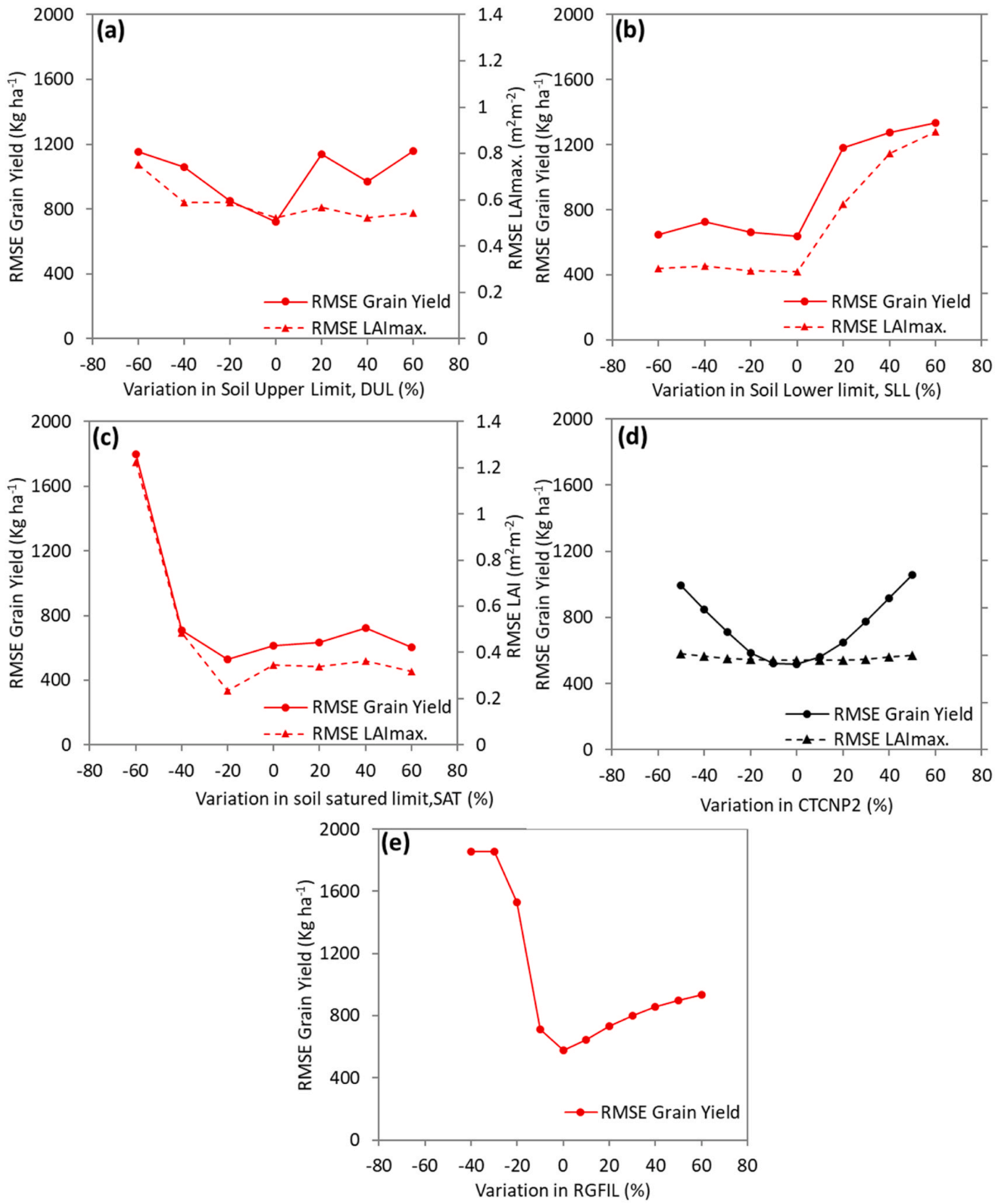

Fig. 6. Sensitivity analysis of maize grain yield and maximum leaf area index to the variation (%) in: (a) soil drained upper limit (DUL); (b) soil lower limit (SLL); (c) soil saturated limit (SAT); (d) soil nutrient stress factor (CTCNP2); and (e) temperature effect on relative grain filling rate (RGFIL). Sensitivity analysis to DUL, SLL, SAT and RGFIL was done using DI2019 and DI2020 treatments; and Sensitivity analysis to CTCNP2 was done using DN2018 and DN2019 treatments.

validation process.

A CTCNP2 value of 0.12 depicted at best the nutrient stress level as the RMSE of the grain yield and $LAI_{max.}$ were lowest at this point. Low values of CTCNP2 improved model prediction of grain yield likely due to an improved plant nitrogen uptake (Liu et al., 2012; Jiang et al., 2019), resulting in an improved grain yield prediction. However, Tovihoudji et al. (2019) found that the performance of DSSAT in predicting grain yield increased with increased values of CTCNP2. This opposite trend observed in our case study would be probably related to an additional nitrogen stress inherent to the 2019 growing season experiment, where a heavy rainfall event (90 mm) was recorded few days after application of NPK (Fig. 1A2). The heavy rainfall event would have resulted in nitrogen leaching and lower nitrogen uptake by plant. The lower values of the CTCNP2 would have improved overall nutrient uptake by crops, thereby improving yield predictions.

The performance of DSSAT model in predicting crop growth and yield under various irrigation management techniques has been widely assessed (Malik et al., 2019; Bai et al., 2022; Jiang et al., 2016), but very few studies were conducted in West Africa (e.g see Atiah et al., 2021). In addition, the model performance has also been extensively assessed under rainfed conditions in detriment of off-season cereal crop production, because maize production is mainly rainfed in the region (Amouzou et al., 2019). Model showed unsatisfactory predictions of phenological stages under water- and nutrient- deficient conditions. Moreover, the predicted grain yield was similar among DI_0, DI_{25} and DI_{50} during the calibration and between DI_0 and DI_{25} treatments during the validation process. The similar predicted grain yield among DI treatments, may have resulted from the similar predicted phenological

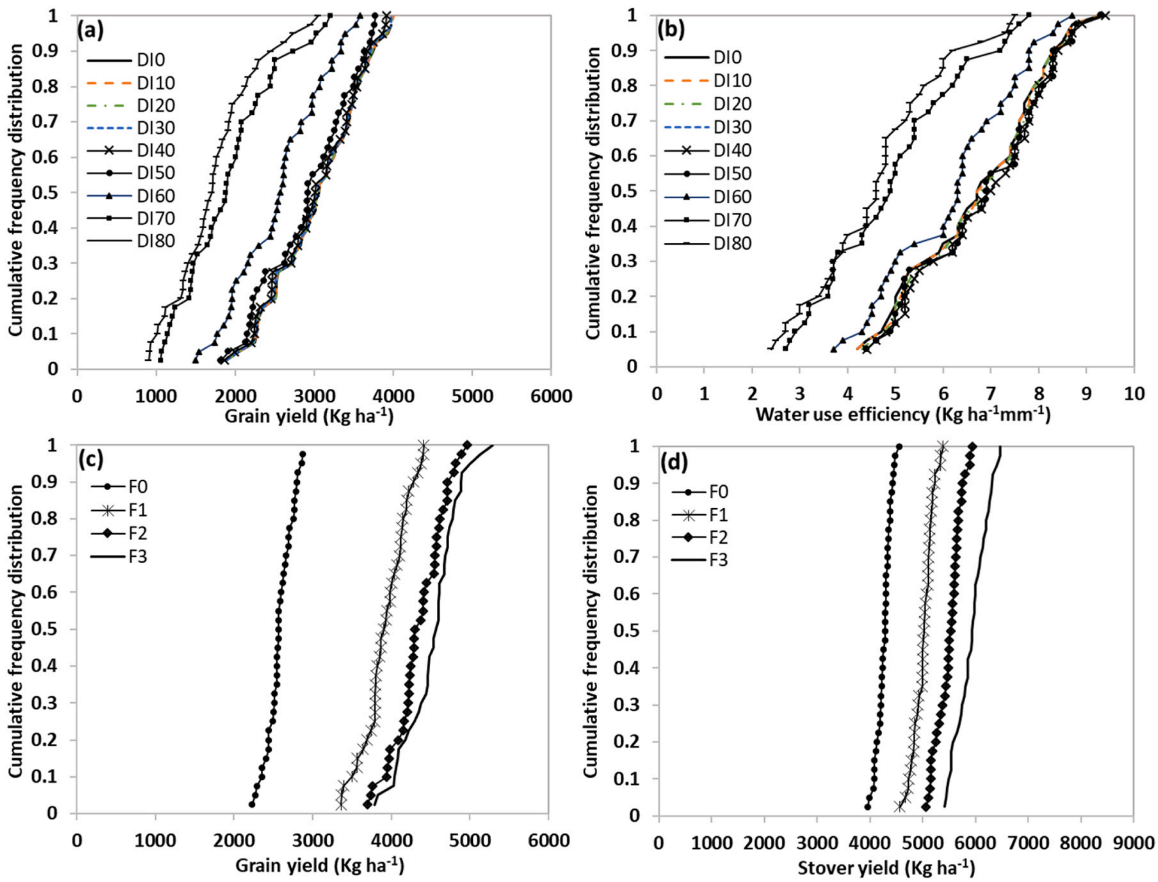

Fig. 7. Cumulative probability distribution for (a) grain yield and (b) maize water use efficiency under deficit irrigation scenarios; and for (c) grain and (b) stover yields under deficit nutrient scenarios using historical weather dataset from 1980 to 2019 in Parakou.

stages among DI treatments. In fact, evidence showed that the contribution of crop cultivar coefficients to grain yield and LAI decreases significantly under water stress conditions (Corbeels et al., 2016).

4.1.1. Model evaluation

The calibration phase of DSSAT revealed that the model is limited in the definition of phenological stages. The predicted anthesis and maturity dates were identical among treatments during the same growing seasons, implying that the DSSAT model did not differentiate these phenological dates among optimal treatments (water stress or fertilizer) and stress treatments. Indeed, DSSAT defines crop phenological stages based on the cumulated degree days, which was identical among treatments during the same growing season (Table 3). In addition, the phenology of crops is solely influenced by temperature or thermal time in DSSAT (Dhakar et al., 2018). Thus, DSSAT model does not account for the effect of stress, being water or fertilizer during the computation of crop phenological stages. This limitation in DSSAT, was also pointed out by Song and Jin, (2020), who observed that the model simulated similar phenological dates among water stress treatments. Thus, the model needs further improvement to integrate the effect of stresses such as water or nutrient stress on crop phenology.

4.2. Long term scenario analysis and Implications

The maize WUE increases by 2 % with the application of DI_{40} deficit irrigation, relative to optimal irrigation application (Fig. 8), suggesting that the crop WUE increases with deficit irrigation. These findings are consistent with those of Dejonge et al., (2012) who reported that simulated WUE of maize increased with increasing deficit irrigation. According to Fereres and Soriano (2007), the increase of WUE with increase of deficit irrigation is explained by the fact that crop evapotranspiration increases more or less linearly with small amount of irrigation, but this relationship becomes curvilinear at a point whereby an additional increase of irrigation no longer increases crop evapotranspiration since part of the water is lost.

The reduction of 40 % and 60 % of irrigation amount at the vegetative stage guarantees a minimum grain yield of 1869 Kg ha^{-1} and 1500 respectively. The scenario analyses revealed that the reduction of the irrigation amount by 40 % generates similar grain yield with the optimal irrigation scenario, while reducing irrigation rates by 60 % induces similar crop WUE as with the optimal irrigation application. These results suggest that increase of crop WUE under deficit irrigation is not linearly related to grain yield. In fact, a compromise must be made to identify the irrigation rate that would simultaneously minimize yield loss and increase crop WUE.

5. Conclusion

Off-season crop production could be beneficial for improving food security in West Africa countries. However, there is scanty information on optimal use of water and fertilizer resources for off-season crop production. This study provided findings on this gap. The DSSAT crop model was calibrated and validated to simulate the effect of deficit irrigation on maize growth and yields under different nutrient deficit rates during the off-season. The calibration of maize genetic coefficients resulted in a better prediction of the dates to anthesis and to maturity in the nutrient deficit treatments, unlike in the deficit irrigation treatments; although, these phenological dates were identical among the nutrient deficit treatments or the deficit irrigation treatments. The model did not account for the effect of water or nitrogen stress in the

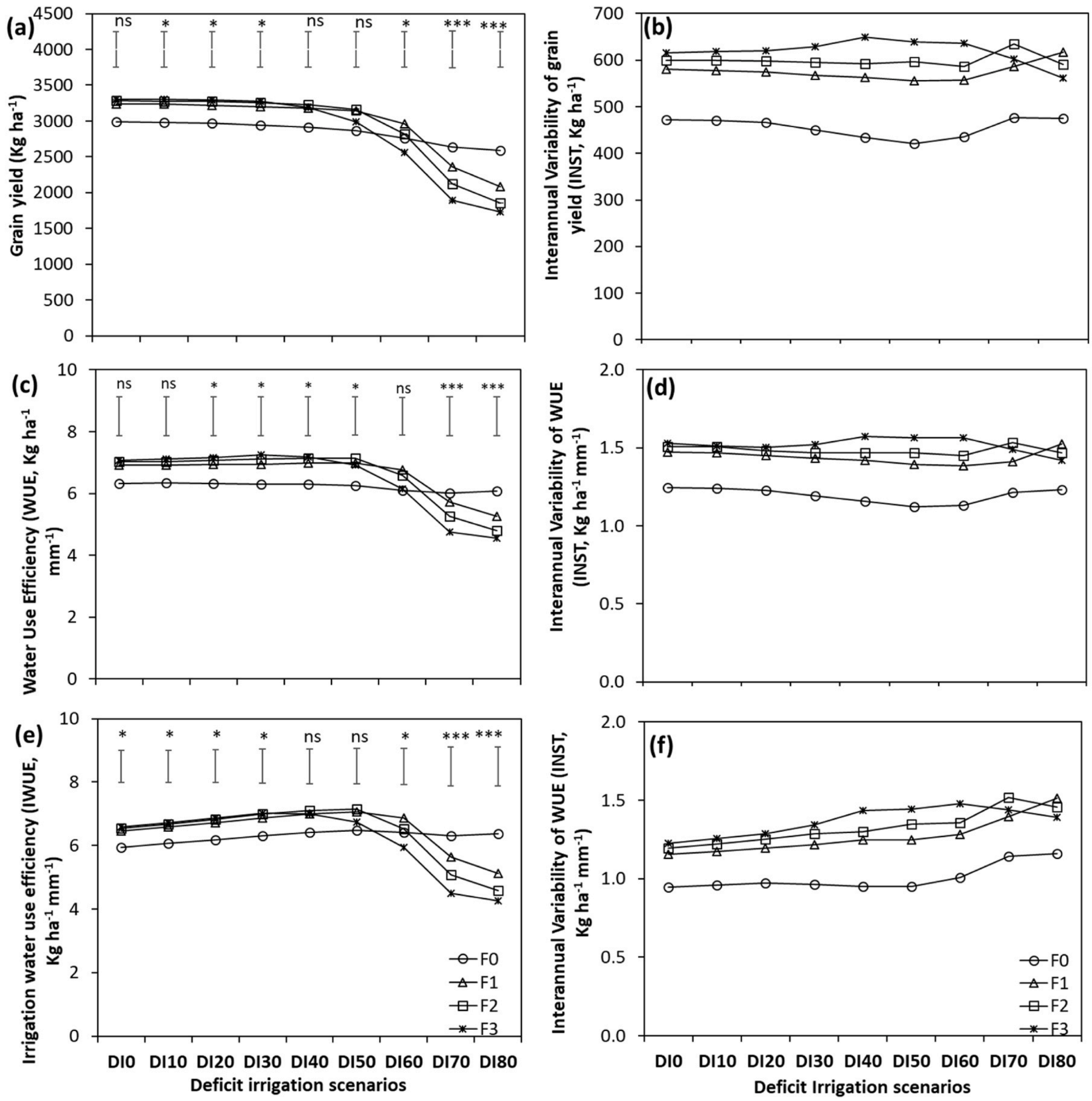

Fig. 8. Simulated average values and Inter-annual variability of maize grain yield (a, b), WUE (c, d) and IWUE (e, f) in response to the combined deficit irrigation (DI_0 to DI_{80}) and deficit nutrient (F_0 to F_3) over 40 years (1980–2019) period.

determination of phenological dates, and also demonstrated a low contribution of the phenological dates to the prediction of LAI and grain yield. This study showed that reducing the crop water requirements by 40–60 % at the vegetative stage and combining it with the recommended fertilizer rates, half of the recommended fertilizer rates or one-third of the recommended fertilizer rates, guarantees an optimal grain yield and simultaneously ensures higher WUE and IWUE. These combined irrigation and fertilizer rates also offer medium inter-annual stability of these variables. Findings suggest that improvements of the model are required to adequately represent the effect of any abiotic stress on crop phenology, and to improve the contribution of phenological dates to the prediction of crop LAI and yield.

Funding

This work was supported by the "Académie de Recherche et d'Enseignement Supérieur" (ARES), Award number 2019-MAA-963 and 2020-MAA-413; and the "Union Economique et Monétaire Ouest Africaine" (UEMOA), Edition 2019–2020.

CRediT authorship contribution statement

P.B. Irénikatché Akponikpè: Visualization, Validation, Supervision, Methodology, Funding acquisition, Conceptualization. **Charles L. Bielders:** Methodology, Funding acquisition, Conceptualization, Data curation, Validation, Visualization. **M. Gloriose B. Allakonon:** Writing – original draft, Visualization, Funding acquisition, Formal analysis, Data curation, Conceptualization. **Pierre G. Tovihoudji:** Methodology, Formal analysis.

Declaration of Competing Interest

The authors declare that they have no known competing financial interests or personal relationships that could have appeared to influence the work reported in this paper.

Appendix A. Supporting information

Supplementary data associated with this article can be found in the online version at doi:10.1016/j.fcr.2024.109613.

Data availability

Data will be made available on request.

References

Adnan, A.A., Jibrin, J.M., Kamara, A.Y., Abdulrahman, B.L., Shaibu, A.S., 2017. Using CERES-Maize model to determine the nitrogen fertilization requirements of early maturing maize in the Sudan Savanna of Nigeria. J. Plant Nutr. 40, 1066–1082. https://doi.org/10.1080/01904167.2016.1263330.

Agbossou, E.K., Toukon, C., Akponikpè, P.B.I., Afouda, A., 2012. Climate variability and implications for maize production in Benin: A stochastic rainfall analysis. Afr. Crop Sci. J. 20 (2), 493–503.

Allakonon, M.G.B., Akponikpè, P.B.I., 2022a. Relationship of maize yield to climatic and environmental factors under deficit irrigation: a quantitative review. Int. *J. Agron.* 2022. https://doi.org/10.1155/2022/2408439.

Allakonon, M.G.B., Zakari, S., Tovihoudji, P.G., Fatondji, A.S., Akponikpè, P.B.I., 2022b. Grain yield, actual evapotranspiration and water productivity responses of maize crop to deficit irrigation: A global meta-analysis. Agr. Water Manag. 270, 107746. https://doi.org/10.1016/j.agwat.2022.107746.

Allé, C.S.U.Y., Baron, C., Guibert, H., Agbossou, E.K., Afouda, A.A., 2014. Choice and risks of management strategies of agricultural calendar: application to the maize cultivation in south Benin. Int. J. Innov. Appl. Stud. 7 (3), 1137–1147.

Amouzou, K.A., Naab, J.B., Lamers, J.P.A., Becker, M., 2018. CERES-Maize and CERES Sorghum for modeling growth, nitrogen and phosphorus uptake, and soil moisture dynamics in the dry savanna of West Africa. Field Crops Res 217, 134–149. https://doi.org/10.1016/j.fcr.2017.12.017.

Amouzou, K.A., Lamers, J.P.A., Naab, J.B., Borgemeister, C., Vlek, P.L.G., Becker, M., 2019. Climate change impact on water- and nitrogen-use efficiencies and yields of maize and sorghum in the northern Benin dry savanna, West Africa. Field Crops Res 235, 104–117. https://doi.org/10.1016/j.fcr.2019.02.021.

Anapalli, S.S., Ahuja, L.R., Ma, L., Timlin, D.J., Stockle, C.O., Boote, K.J., Hoogenboom, G., 2008. Current Water Deficit Stress Simulations in Selected Agricultural System Simulation Models. In: Ahuja, L.R., Reddy, V.R., Saseendran, S. A., Yu, Q. (Eds.), Response of Crops to Limited Water: Understanding and Modeling Water Stress Effects on Plant Growth Processes, pp. 1–38.

Atiah, W.A., Amekudzi, L.K., Akum, R.A., Quansah, E., Antwi-Agyei, P., Danuor, S.K., 2021. Climate variability and impacts on maize (*Zea mays*) yield in Ghana, West Africa. Q. J. R. Meteorol. Soc. 148 (742), 185–198. https://doi.org/10.1002/qj.4199.

Badabaté, D., Koffi, H., Kpékourma, W., Komlan, B., Thierry, T., Koffi, A., 2012. Agriculture de contre saison sur les berges de l'OTI et ses affluents. Afr. Crop Sci. J. 20 (s2), 613–624.

Bai, Y., Yue, W., Ding, C., 2022. Optimize the irrigation and fertilizer schedules by combining DSSAT and genetic algorithm. Environ. Sci. Pollut. Res 29, 52473–52482. https://doi.org/10.1007/s11356-022-19525-z.

Corbeels, M., Chirat, G., Messad, S., Thierfelder, C., 2016. Performance and sensitivity of the DSSAT crop growth model in simulating maize yield under conservation agriculture, 2016 Eur. J. Agron. 76, 41–53. https://doi.org/10.1016/j.eja.2016.02.001.

DeJonge, K.C., Ascough, J.C., Ahmadi, M., Andales, A.A., Arabi, M., 2012. Global sensitivity and uncertainty analysis of a dynamic agroecosystem model under different irrigation treatments. Ecol. Model. 231, 113–125.

Dhakar, R., Chandran, M.A.S., Nagar, S., Kumari, V.V., Subbarao, A.V.M., Bal, S.K., Kumar, P.V., 2018. Field crop responses to water stress: Assessment through Crop Models. In: Bal, S.K., et al. (Eds.), Advances in Crop Environment Interaction, pp. 287–315. https://doi.org/10.1007/978-981-13-1861-0_11.

Dhillon, M.S., Dahms, T., Kuebert-Flock, C., Borg, E., Conrad, C., Ullmann, T., 2020. Modelling Crop Biomass from Synthetic Remote Sensing Time Series: Example for the DEMMIN Test Site, Germany. Remote Sens 12, 1819. https://doi.org/10.3390/rs12111819.

Direction Générale de l'Environnement et du Climat, (D.G.E.C.), 2022. Plan Natl. D. 'Adapt. Aux. Chang. Clim. du Bénin 175.

Dzotsi, K., Agboh-Noameshie, A., Struif Bontkes, T.E., Singh, U., Dejean, P., Wopereis, M. C.S., 2003. Using DSSAT to derive optimum combinations of cultivar and sowing date for maize in Southern Togo. In: Bontkes, T.E., Wopereis, M.C.S. (Eds.), Decision Support Tools for Smallholder Agriculture in Sub-Saharan Africa: A Practical Guide. Chapter, 7, pp. 100–113.

FAO, 1992. CROPWAT: A computer program for irrigation planning and management. FAO Irrig. Drain. 123.

Fereres, E., Soriano, M.A., 2007. Deficit irrigation for reducing agricultural water use. J. Exp. Bot. 58 (2), 147–159. https://doi.org/10.1093/jxb/erl165.

Gadédjisso-Tossou, A., Avellan, T., Schütze, N., 2018. Potential of deficit and supplemental Irrigation under climate variability in Northern Togo, West Africa. Water 10, 1803. https://doi.org/10.3390/w10121803.

Geerts, S., Raes, D., 2009. Deficit irrigation as on-farm strategy to maximize crop water productivity in dry areas. Agr. Water Manag. 96, 1275–1284. https://doi.org/10.1016/j.agwat.2009.04.009.

Geng, S.M., Yan, D.H., Yhang, Z.B., Wang, Z.L., Girmad, A., 2017. Performance assessment and application of the DSSAT-CERES Maize model for simulating maize yield under water stress conditions. IOP Conf. Series: Earth and Environmental Science 82, 012030. 3rd International Conference on Water Resource and Environment (WRE 2017). ⟨https://doi.org/10.1088/1755-1315/82/1/012030⟩.

Gijsman, A.J., Hoogenboom, G., Parton, W.J., Kerridge, P.C., 2002. Modifying DSSAT crop models for low-input agricultural systems using a soil organic matter–residue module from CENTURY. Agron. J. 94, 462–474. https://doi.org/10.2134/agronj2002.4620.

Godwin, D.C., Singh, U., 1998. Nitrogen balance and crop response to nitrogen in upland and lowland cropping systems. In: Tsuji, G., Hoogenboom, Y.G., Thorton, P.K. (Eds.), Understanding Options for Agricultural Production. Kluwer Academic Publishers, The Netherlands, pp. 55–77.

Gomaa, M.A., Kandil, E.E., El-Dein, A.A.M.Z., Abou-Donia, M.E.M., Ali, H.M., Abdelsalam, N.R., 2021. Increase maize productivity and water use efficiency through application of potassium silicate under water stress. Sci. Rep. 11, 224. https://doi.org/10.1038/s41598-020-80656-9.

Hoogenboom, G., Porter, C.H., Shelia, V., Boote, K.J., Singh, U., White, J.W., Hunt, L.A., Ogoshi, R., Lizaso, J.I., Koo, J., Asseng, S., Singels, A., Moreno, L.P., Jones, J.W., 2019. Decision Support System for Agrotechnology Transfer (DSSAT) Version 4.7 (www.DSSAT.net). Decision Support System for Agrotechnology Transfer (DSSAT) Version 4.7 (www.DSSAT.net). DSSAT Foundation, Gainesville, Florida, USA.

Igué, A.M., Adjanohoun, A., Saidou, A., Ezui, G., Attiogbe, P., Kpagbin, G., Gotoechan-Hodonou, H., Youl, S., Pare, T., Balogoun, I., Ouedraogo, J., Dossa, E., Mando, A., Sogbedji, J.M., 2013. Application et adaptation de l'approche intégrée DSSAT-SIG à la formulation des doses d'engrais pour la culture du maïs au Sud et au Centre du Bénin. Bull. Rech. Agron. Bénin BRAB (Numéro Spécial Fertilité du maïs.) 24–33.

Jiang, R., He, W., Zhou, W., Hou, Y., Yang, J.Y., He, P., 2019. Exploring management strategies to improve maize yield and nitrogen use efficiency in northeast China using the DNDC and DSSAT models. Comput. Electron. Agric. 166, 104988. https://doi.org/10.1016/j.compag.2019.104988.

Jiang, Y., Zhang, L., Zhang, B., He, C., Jin, X., Bai, X., 2016. Modeling irrigation management for water conservation by DSSAT-maize model in arid northwestern China. Agr. Water Manag. 177, 37–45. https://doi.org/10.1016/j.agwat.2016.06.014.

Jones, J.W., Hoogenboom, G., Porter, C.H., Boote, K.J., Batchelor, W.D., Hunt, L.A., Wilkens, P.W., Singh, U., Gijsman, A.J., Ritchie, J.T., 2003. The DSSAT cropping system model. Eur. J. Agron. 18, 235–265. https://doi.org/10.1016/S1161-0301(02)00107-7.

Jones, C.A., Kiniry, J.R., 1986. CERES-MAIZE: A simulation Model of Maize Growth and Development. CERES-MAIZE: A simulation Model of Maize Growth and Development. Texas A&M University Press, College Station, TX, p. 198.

Jones, J.W., Boote, K.J., Hoogenboom, G., Jagtap, S.S., Wilkerson, G.G., 1989. SOYGRO V5.42, Soybean Crop Growth Simulation Model. User's Guide. Fl. Agric. Exp. Sta. University of Florida, Gainesville, p. 53.

Jones, P.G., Thornton, P.K., 2003. The potential impacts of climate change on maize production in Africa and Latin America in 2055. Glob. Environ. Change 13, 51–59.

Kapetch, P., Sakai, K., Pisanjaroen, K., Sansayawichai, T., Cho, T., Nakamura, S., Nakandakari, T., 2016. Calibration and validation of two crop models for estimating sugarcane yield in northeast Thailand. Trop. Agr. Dev. 60 (1), 31–39.

Liu, H.-L., Yang, J.-y, Ping, H.E., Bai, Y.-L., Jin, J.-Y., Drury, C.F., Zhu, Y.-P., Yang, X.-M., Li, W.-J., Xie, J.-G., Yang, J.-M., Hoogenboom, G., 2012. Optimizing Parameters of CSM-CERES-Maize Model to Improve Simulation Performance of Maize Growth and Nitrogen Uptake in Northeast China. J. Integr. Agric. 11 (11), 1898–1913.

Ma, H., Malone, R.W., Jiang, T., Yao, N., Chen, S., Song, L., Feng, H., He, J., 2020. Estimating crop genetic parameters for DSSAT with modified PEST software. Eur. J. Agron. 115, 126017. https://doi.org/10.1016/j:eja.2020.126017.

Ma, L., Hoogenboom, G., Saseendran, S.A., Bartling, P.N.S., Ahuja, L.R., Green, T.R., 2009. Effects of Estimating Soil Hydraulic Properties and Root Growth Factor on Soil Water Balance and Crop Production. Agron. J. 101, 572–583. https://doi.org/10.2134/agronj2008.0206x.

Ma, L., Ahuja, L., Saseendran, S., Malone, R., Green, T., Nolan, B., Bartling, P., Flerchinger, G., Boote, K., Hoogenboom, G., 2011. A protocol for parameterization and calibration of RZWQM2 in field research. Methods Introd. Syst. Models into Agric. Res. 2, 1–64.

Malik, W., Isla, R., Dechmi, F., 2019. DSSAT-CERES-maize modelling to improve irrigation and nitrogen management practices under Mediterranean conditions. Agr. Water Manag. 213, 298–308. https://doi.org/10.1016/j.agwat.2018.10.022.

McCarthy, D.S., Vlek, P.L.G., Fosu-Mensah, B.Y., 2012. The Response of maize to N fertilization in a sub-humid region of Ghana: understanding the processes using a crop simulation model. In: Kihara, J., Fatondji, D., Jones, J.W., Hoogenboom, G., Tabo, R., Bationo, A. (Eds.), Improving Soil Fertility Recommendations in Africa Using the Decision Support System for Agrotechnology Transfer (DSSAT). Springer, Netherlands, pp. 61–75. https://doi.org/10.1007/978-94-007-2960-5_5.

MEPN, 2008. Ministère de l'Agriculture, de l'Elevage et de la Pêche). Carte du Bénin Pr. ésentant Les. zones agroécologiques.

Priesack, E., Gayler, S., Hartmann, H.P., 2006. The impact of crop growth sub-model choice on simulated water and nitrogen balances. Nutr. Cycl. Agroecosyst 75, 1–13.

Priestley, C.H.B., Taylor, R.J., 1972. On the assessment of surface heat flux and evaporation using large scale parameters. Mon. Weather Reviz 100 (2), 81–92.

Song, L., Jin, J., 2020. Improving CERES-Maize for simulating maize growth and yield under water stress conditions. Eur. J. Agron. 117, 126072. https://doi.org/10.1016/j.eja.2020.126072.

Tidjani, M.A., Akponikpè, P.B.I., 2012. Evaluation des stratégies paysannes d'adaptation aux changements climatiques: cas de la production du maïs au Nord-Bénin. Afr. Crop Sci. J. 20 (s2), 425–441.

Tofa, A.I., Chiezey, U.F., Babaji, B.A., Kamara, A.Y., Adnan, A.A., Beah, A., Adam, A.M., 2020. Modeling Planting-Date Effects on Intermediate-Maturing Maize in Contrasting Environments in the Nigerian Savanna: An Application of DSSAT Model. Agronomy 10, 871. https://doi.org/10.3390/agronomy10060871.

Tovihoudji, P.G., Akponikpè, P.B.I., Agbossou, E.K., Bielders, C.L., 2019. Using the DSSAT Model to support Decision making regarding fertilizer microdosing for maize production in the Sub-humid region of Benin. Front. Environ. Sci. 7, 13. https://doi.org/10.3389/fenvs.2019.00013.
United Nations, 2009. World's Population Prospects. World's Population Prospects. United Nations.
USDA-Soil Conservation Service, 1972. Soil series of the United States, Puerto Rico and the Virgin Islands: their taxonomic classification, 436. Supplement to Agricultural Handbook No, Washington, DC.
Willmott, C.J., 1981. On the validation of models. Phys. Geogr. 2, 184–194.
Yabi, I., Afouda, F., 2012. Extreme rainfall years in Benin (West Africa). Quat. Int. 262, 39–43. https://doi.org/10.1016/j.quaint.2010.12.010.
Yang, J.M., Yang, J.Y., Liu, S., Hoogenboom, G., 2014. An evaluation of the statistical methods for testing the performance of crop models with observed data. Agric. Syst. 127, 81–89. https://doi.org/10.1016/j.agsy.2014.01.008.
Yegbemey, R.N., Yegbemey, E.O., Yabi, J.A., 2017. Sustainability analysis of observed climate change adaptation strategies in maize farming in Benin, West Africa. Outlook Agric. *46* (1), 20–27. https://doi.org/10.1177/0030727016689638.